Available online at www.sciencedirect.com
SCIENCE DIRECT®
Aerospace Science and Technology 8 (2004) 583–590
Aerospace Science and Technology
www.elsevier.com/locate/aescte

Experimental investigation of a pitching airfoil in transonic flow ☆

Experimentelle Untersuchung von Drehschwingungen eines Tragflügelprofils in schallnaher Anströmung

C. Hillenherms *, W. Schröder, W. Limberg

Aerodynamisches Institut der RWTH Aachen, Wüllnerstraße zw. 5 und 7, 52062 Aachen, Germany

Received 24 February 2004; received in revised form 23 April 2004; accepted 1 June 2004

Available online 29 July 2004

Abstract

The interaction of aerodynamic and structural forces on a 2-D rectangular wing section oscillating in pitch at transonic flow is studied experimentally. The investigations include free and forced oscillations. The free pitching motion is generated by a symmetric elastic suspension on both sides of the rigid wing, whereas the forced oscillations are induced by an electric actuator on one side of the model. The investigations are based on the simultaneously measured surface pressures and aerodynamic forces while the wing section is oscillating in pitch. The wing model is oscillating about mean incidence angles of zero to two degrees at Mach numbers of 0.50 to 0.85, corresponding to Reynolds numbers 1.5 to 2.2 million. The wing has a supercritical BAC 3-11/RES/30/21 airfoil with a relative thickness of 11% [I.R.M. Moir, AGARD-AR-303, DRA, Farnborough, 1994]. Preliminary investigations include measurements of the steady pressure distribution and flow visualisation at transonic Mach numbers for a fixed mounted wing model with the same airfoil.

Zusammenfassung

Zur Untersuchung der Strömungs-Struktur-Wechselwirkung an einem Profilmodell werden freie und vorgegebene Drehschwingungen in schallnaher Anströmung durchgeführt. Freie Drehschwingungen werden mittels beidseitiger, elastischer Lagerung des starren Profilmodells generiert, die ausschließlich Änderungen des Anstellwinkels erlaubt. Schwingungen mit vorgegebener harmonischer Bewegung bei variabler Frequenz und Amplitude werden durch einen elektrischen Antrieb auf einer Seite des Modells erzeugt. Es werden jeweils die instationäre Druckverteilung, die Auflagerkräfte und das Torsionsmoment sowie der momentane Anstellwinkel gleichzeitig erfaßt. Die Versuche werden bei mittleren Anstellwinkeln zwischen 0° und 2° und Machzahlen von 0.50 bis 0.85 durchgeführt, dies entspricht Reynoldszahlen von 1.5 bis 2.2 Millionen. Die überkritische Profilgeometrie BAC 3-11/RES/30/21 [I.R.M. Moir, AGARD-AR-303, DRA, Farnborough, 1994] weist eine relative Dicke von 11% auf. Zur Untersuchung der stationären Strömungszustände wurden zuvor bei ebenfalls schallnaher Anströmung am fest eingespannten Profilmodell die Druckverteilung gemessen und Versuche zur Strömungssichtbarmachung durchgeführt.

Keywords: Unsteady; Transonic; Two-dimensional; Supercritical airfoil; Pitch oscillations

Schlüsselwörter: Instationär; Transsonisch; Zweidimensional; Superkritisches Profil; Drehschwingungen

☆ This article was presented at the German Aerospace Congress 2002.

* Corresponding author. Current address: Airbus Deutschland GmbH, Kreetslag 10, D-21129 Hamburg, Germany, Tel.: +49-(0)40-743-86174; fax.: +49-(0)40-743-81235.

E-mail address: Cornelia.Hillenherms@airbus.com (C. Hillenherms).

1270-9638/$ – see front matter
doi:10.1016/j.ast.2004.07.001

Nomenclature

a	speed of sound
b	airfoil span
c	airfoil chord
$c_{l,L}$	lift coefficient (local, global)
$c_{m,M}$	moment coefficient about $c/4$ (local, global)
c_p	pressure coefficient
f	frequency
I	moment of inertia
K_α	torsional stiffness
M_α	pitching moment about $c/4$ (+ nose up)
Ma_∞	freestream Mach number
Re	Reynolds number
u_∞	freestream velocity
α	angle of attack (+ nose up)
$\hat{\alpha}$	amplitude of Pitch motion
$\alpha(t)$	Pitch motion
$\ddot{\alpha}(t)$	Pitch acceleration
δ	decaying constant
ϑ	damping ratio
$\omega_\alpha = 2\pi f_\alpha$	Pitch angular frequency
$\omega^* = \omega_\alpha c/u_\infty$	reduced frequency, based on chord length c

Sub- and superscripts

$(y)'$	fluctuating component
$\bar{y}$	mean value
$\mathcal{R}(z)$	real part of a complex quantity
$\mathcal{I}(z)$	imaginary part of a complex quantity
$_\alpha$	quantity related to pitch motion

1. Introduction

The prediction of stability boundaries is one of the most essential tasks in today's aircraft design process mainly due to the extended use of lightweight structures. As a consequence, efficient design tools have to be developed that are based on numerical simulations of the fluid–structure interaction. This is particularly demanding in the case of transonic flow where non-linear effects are playing an important role. However, the development of reliable aeroelastic codes requires experimental data to assess the accuracy and validity of the computed results. Besides the validation of numerical methods, the experiments serve for the study of physical phenomena like shock/boundary-layer interaction.

The general objective of this work is thus to deliver and to analyse new, steady and unsteady data in the two-dimensional domain of an oscillating supercritical wing section with one degree-of-freedom under approximately free-flight conditions. Steady data are used as a reference to interpret the unsteady results, particularly with respect to the location of separation areas and shock positions. Results from decaying pitch oscillation tests serve to analyse the damping as well as the phase relations of the aerodynamic forces with respect to the oscillatory motion of the airfoil. Moreover forced oscillations at small amplitudes are conducted to analyse the aerodynamic response to a prescribed pitch motion, i.e., to determine the behaviour of the aerodynamic forces in relation to the oscillation of the airfoil.

2. Experimental setup

2.1. Elastic suspension

Fig. 1 shows the model mounting for free pitching motion with an elastic suspension on both sides.

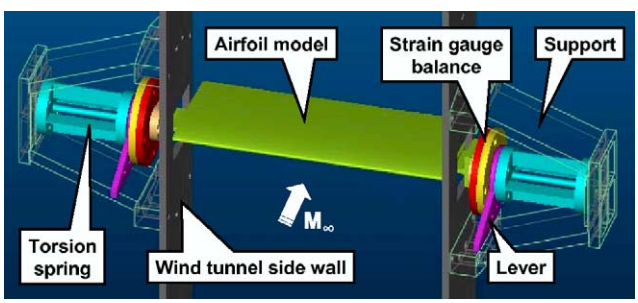

Fig. 1. Elastically mounted rectangular wing section.

The grey panels symbolise the side walls of the test section. Only the airfoil itself is subject to the flow while all parts of the suspension are mounted outside of the test section. For the experiments, these outer parts are sealed with a cover on each side because the test section side panels provide air gaps for the airfoil oscillations. A two-component strain-gauge balance is mounted on both sides of the airfoil model to measure the unsteady forces in the direction of the airfoil chord and perpendicular to it. The torsional moment is measured by means of two symmetrical torsional springs which also serve as an elastic mount and allow the wing to pitch. The torsion springs themselves are fixed to the wall-mounted support. The time-dependent angle of attack of the model is taken on one side of the test section by two laser triangulators pointing on the lever mounted between the balance and the spring. A more detailed description of this setup can be found in Ref. [3].

2.2. External excitation

The torsion springs are removed and replaced by pivoted shafts in order to provide free rotation for the forced pitch oscillations.

An excitation construction is mounted on one side of the test section, consisting of a lever and an adjustable excen-

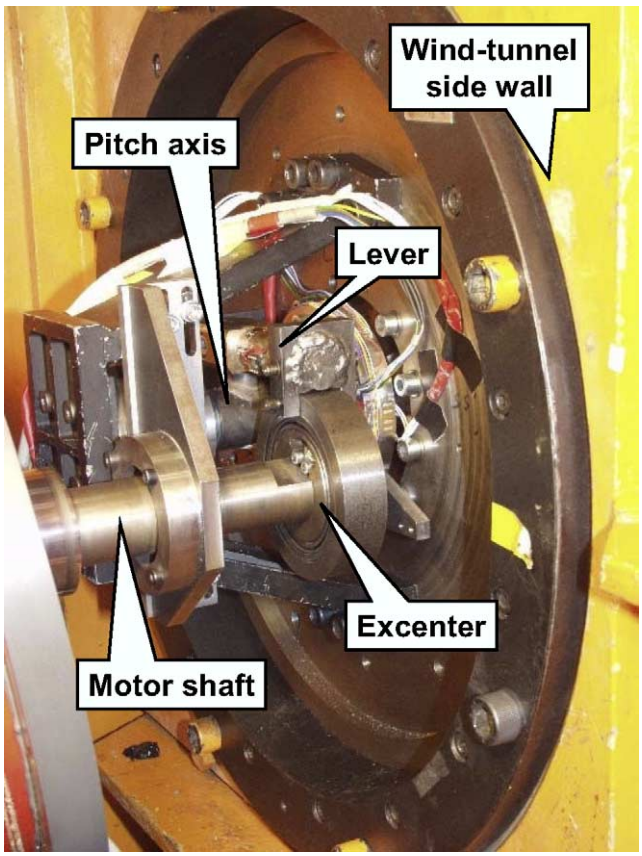

Fig. 2. Scheme of the wing section with eletrical excitation.

ter which is driven by a 5.5 kW asynchronous motor and a frequency converter (Fig. 2). It allows excitation frequencies up to 100 Hz. The pitching motion is again measured by two laser triangulators on the other side of the test section.

2.3. Wind tunnel

The investigations are carried out in the trisonic wind tunnel of the Aerodynamisches Institut. The suction type wind tunnel operates intermittent at atmospheric pressure and temperature, and allows test periods of 2 to 5 seconds. Two test sections each of 0.4×0.4 m^2 are available, either with fixed or with 2-D-adaptive walls.

The test section with adaptive upper and lower walls allows measurements in transonic flow [6] with minimum wall interference. The flexible walls are made of spring steel plates clamped to 24 traversing stages with stepping motors (Fig. 3). The wall contours are calculated using the linearised theory for compressible flows and Cauchy's integral formula based on the measured wall pressure distribution and the wall contour [1].

Even for unsteady investigations, a steady adaptation of the walls reduces a large amount of wall interference effects and only residual interferences have to be corrected [10] on the basis of measured unsteady wall pressures. For this purpose, each of the adaptive walls is equipped with 13 additional pressure sensors. However, for the present measurements, a correction of the residual unsteady wall interferences was not performed.

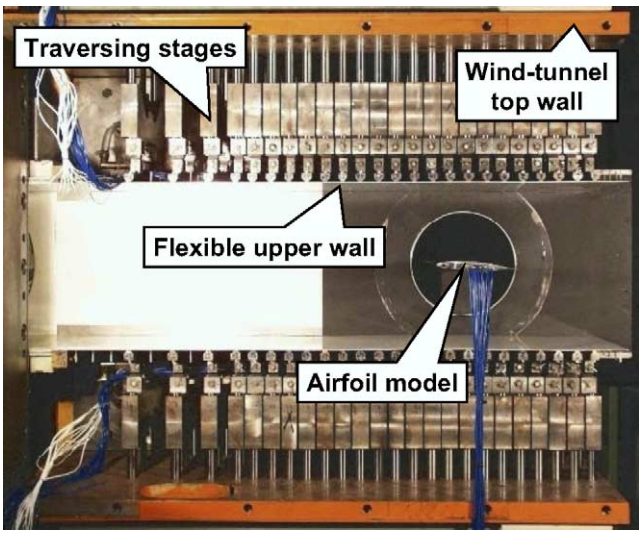

Fig. 3. Adaptive test section.

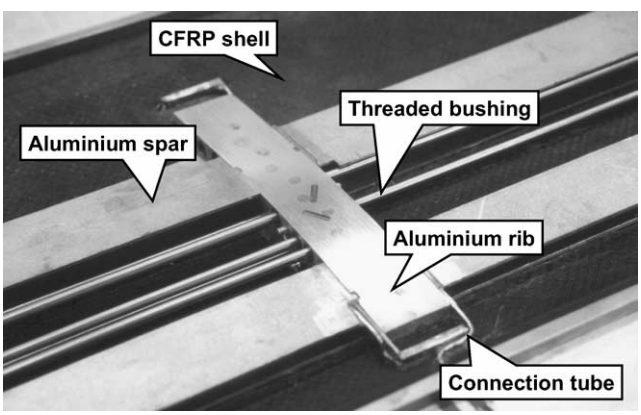

Fig. 4. Upper shell of the second model with central rib, spars and some of the threaded bushings.

2.4. Airfoil model

Three models have been built for the 2-D investigations, two of them for the unsteady tests, and one for the steady tests. The latter will not be described in the following. All models have identical geometries with $c = 150$ mm chord and $b = 400$ mm span. The first model for unsteady testing was used for the decaying oscillations whereas the second one was used for the forced oscillations. Both are made of carbon fiber reinforced plastics to ensure minimum inertial forces and moments. The first one is equipped with eleven, the second one with thirty sub-miniature pressure sensors in the mid-span (Fig. 4). More details of the sensor mounting in that last model are given in Section 2.5. Bending stiffness is obtained by glass fiber and aluminium spars, respectively, whereas the shells contribute the major part of the torsional stiffness of the model. Aluminium and steel flanges, respec-

tively, on either side are necessary to transmit the forces and moments, and to bolt the model to the other devices.

2.5. Pressure measurement technique

The wind tunnel model is equipped with piezo-resistive pressure sensors to record the pressure signals as near to their origins as possible. The cylindrical sensors are mounted into an aluminium rib inside the model with special threaded bushings (Fig. 4). The fixation and the sealing of the sensors are achieved by screwing them into the central rib together with O-rings, leaving only a very small cavity in front of the sensor head and a connection to the surface pressure taps of 0.3 mm diameter. Only the sensors at the leading edge and at the most aft position had to be connected to the surface pressure taps by longer tubes because of the restricted space in the model.

2.6. Force measurement technique

The unsteady forces are measured by a strain-gauge balance made out of maraging steel which is particularly suited for the construction of strain gauge balances due to its extremely high yield strength [5]. It consists of two pairs of circular panels, see Fig. 5, mounted on both sides of the airfoil model in the case of free oscillations.

In the case of forced oscillations only one pair is used on the excitation side since on the other side it would represent only an additional inertia. One panel of each pair is to measure the forces in the chordwise (tangential) direction, whereas the other panel measures the forces perpendicular (normal) to the model chord. The panels have bending beams equipped with strain-gauges to register the beam deformation caused by an acting force. The calibration has confirmed that the balance design provides minimum interference of the different stress modes and minimum sensitivity to torsion. The (static) calibration of the force measurement chain yielded a sensitivity of min. 4 mV/N for normal forces and min. 25 mV/N for tangential forces.

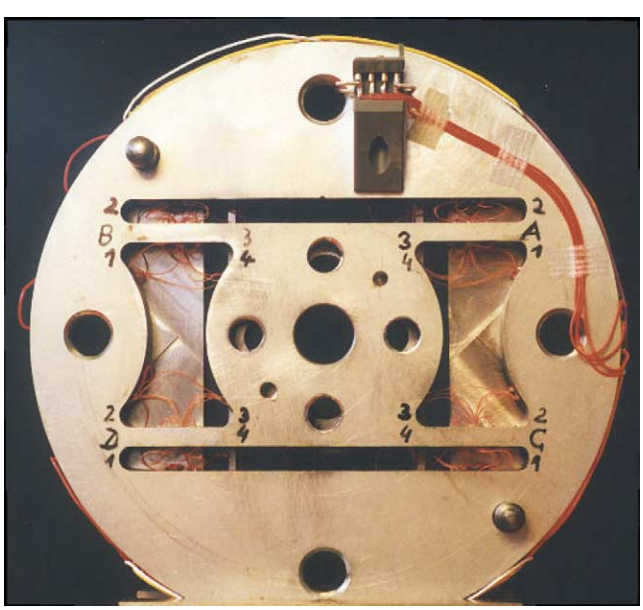

Fig. 5. One balance pair with normal force panel in front.

The eigenfrequency of the balance was estimated to make sure that it is clearly out of the range of frequencies that will be of interest during the unsteady experiments. The first eigenfrequency amounts to

$$f_1 = \frac{\omega_1}{2\pi} = 56.85(26.94)\ \text{kHz} \tag{1}$$

(the values in parentheses belong to the beams of the tangential force panels) and is hence explicitly beyond the interesting and measurable range of frequencies, which is limited by the carrier frequency of the amplifier, see Section 2.7.

2.7. Data acquisition

The data is sampled simultaneously by an industrial PC with five data acquisition boards. The synchronised boards allow maximum sampling of 40 channels at 1.25 MHz with 12 bit resolution. The pressure signals are low-pass filtered and amplified by DC amplifiers, whereas the strain-gauge signals are processed by a 5 kHz carrier frequency amplifier.

3. Results

3.1. Steady measurements

Fig. 6 shows an overview of the steady data base in terms of the lift coefficient with respect to the Mach number for different angles of attack. Measurements of the steady pressure distribution and flow visualisation of the fixed model have been made in the two different test sections and with free (dashed lines) and forced (solid lines) transition, respectively.

The thin lines show measurements with parallel walls while the thick lines pertain to measurements with adapted

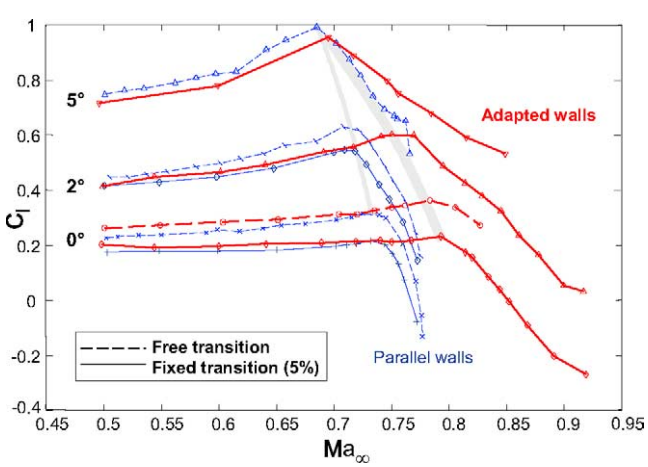

Fig. 6. Measured lift coefficients for transonic Mach numbers and different angles of attack, with free and forced transition at 5% chord, with parallel and adapted walls.

walls. It can be stated that the Mach number envelope is clearly enhanced by wall adaptation, and that the maximum lift coefficients and the corresponding Mach numbers are shifted towards higher values for all measured angles of attack.

Numerical Calculations with the Euler–boundary-layer method MSES [2] have been done in order to complement the experimental database and to get an extended survey of the airfoil flow development. The comparison of the measured and calculated pressure distributions yields a very good agreement for most of the flow cases. An example is presented in Fig. 7 for a Mach number of 0.80, and an angle of attack of $\alpha = 2^\circ$ with a large supersonic area on the upper side of the airfoil and a shock-induced/trailing edge separation. Of course the perturbation effect of the transition strips at 5% profile chord is not reproduced since the strip itself is not modeled in the calculation. Furthermore the numerical method fails in the area behind the shock due to the massive separation that can also be observed in the shadowgraph for this flow case in Fig. 8.

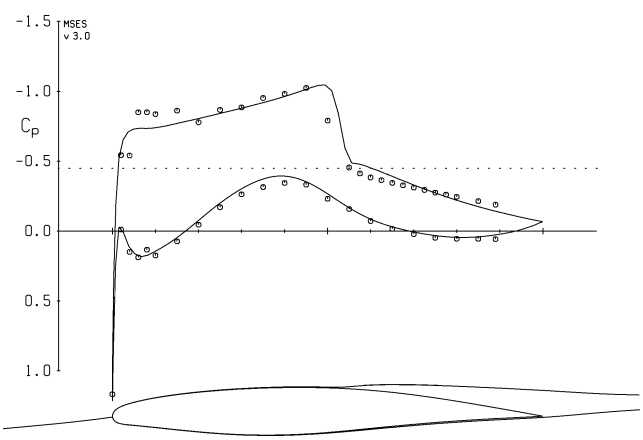

Fig. 7. Comparison of measured (symbols) and calculated (line) pressure distribution for $Ma = 0.80$, $Re = 2.211 \times 10^6$, and $\alpha = 2^\circ$.

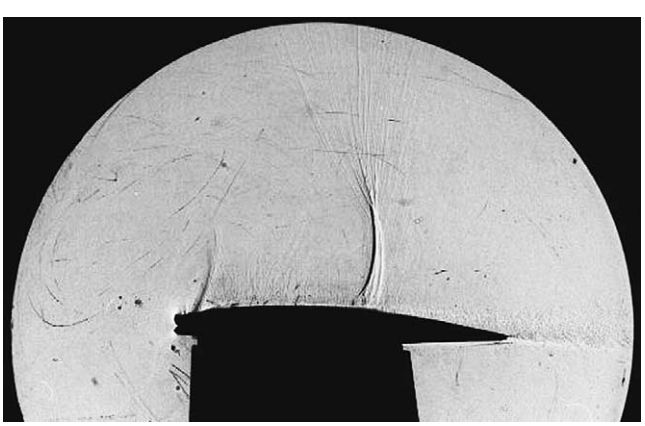

Fig. 8. Shadowgraph for $Ma = 0.80$, and $\alpha = 2^\circ$.

3.2. Unsteady measurements

3.2.1. Decaying pitch oscillations

Decaying and self-sustained pitch oscillations have been carried out at Mach numbers of 0.50 to 0.85 and static angles of attack between 0°, 2°, and 2.5° [4]. The static angle of attack α_{static} is the angle of attack in still air. During the test run, the mean angle of attack adjusts on lower values because of the elastic suspension and the (mean) negative pitching moment. After an initial angular deflection, the model is released under steady flow conditions. The pressure distribution, the reactions, and the instantaneous angle of attack are measured simultaneously.

The pitching motion was decaying in all measured cases, i.e. the damping was always positive, and the system remained stable. Fig. 10 shows the damping coefficient determined from the decaying part of the pitch oscillation (as indicated in Fig. 9) which results in a relatively strong scattering of the values. The different symbols indicate the variation of the static angle of attack. The damping coefficient is increasing for Mach numbers rising from 0.50 to 0.80. But it is steeply decreasing for higher Mach numbers. No reliable statement can be made if this gradient continues until the damping coefficient becomes negative for even higher Mach numbers, since the extent of the supersonic region and the strength of the existing shocks prohibit a reasonable wall adaptation.

A look at the steady measurements, more precisely at the pitching coefficient, leads to a possible interpretation of the trend of the damping distribution. As can be seen in Fig. 11, the slope of the moment coefficient changes at Mach numbers above 0.83 and even becomes positive for $Ma = 0.88$ and $\alpha < 2^\circ$. This may be a hint with respect to the decreasing damping [9].

3.2.2. Forced pitch oscillations

At Mach numbers of 0.50 to 0.85 and mean angles of attack between -1° and 2°, forced pitch oscillations have been carried out with excitation frequencies of 45, 60, and 90 Hz and amplitudes of 0.2° and 0.4°. The reduced frequencies were thus ranging from 0.15 to 0.51. Again the pressure distribution, the reactions, and the pitching motion are measured simultaneously.

Pressure fluctuations on the upper side of the pitching airfoil are displayed in Figs. 12 and 13 for different Mach numbers at a mean angle of attack of -0.5° and two different pitching frequencies of 45 Hz and 90 Hz, respectively, in terms of root-mean-square values. The corresponding reduced frequencies $\omega^* = 2\pi f_\alpha c/u_\infty$ were 0.21–0.15 for $f_\alpha = 45$ Hz and 0.43–0.30 for $f_\alpha = 90$ Hz.

The formation of the shock is represented by the rising levels between the 55% and 65% sensor locations. Slightly higher values can be observed for the higher frequency in the region of the shock.

Furthermore it can be seen that maximum fluctuation levels occur for Mach numbers of 0.72 to 0.77 which is not

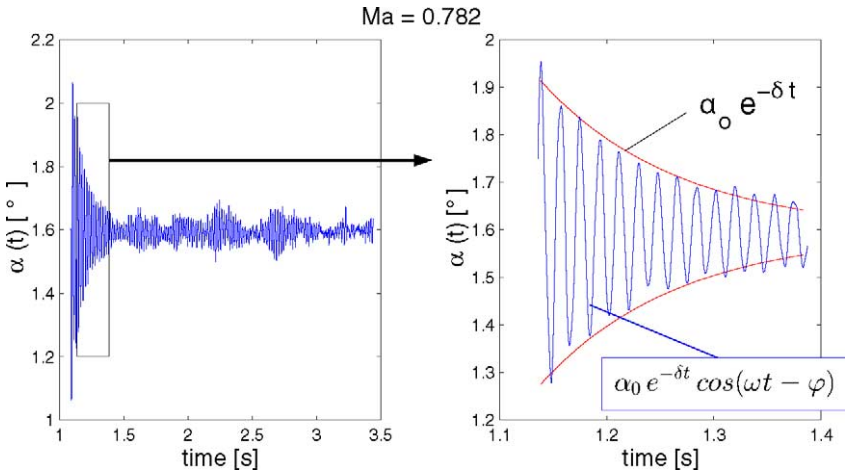

Fig. 9. Typical time record of the pitching motion with enlarged decaying part.

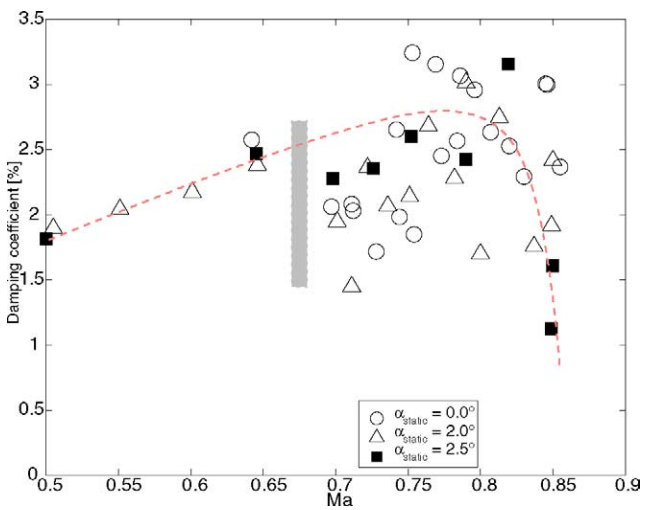

Fig. 10. Damping coefficient with respect to the Mach number.

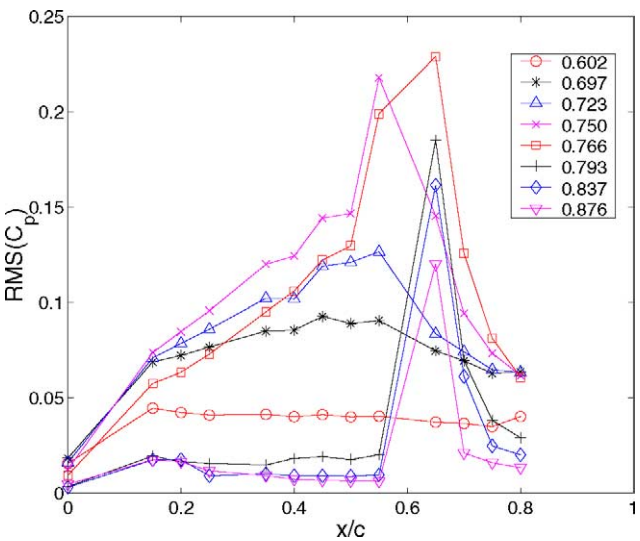

Fig. 12. Fluctuations of the upper surface pressure coefficients for different Mach numbers at $\bar{\alpha} = -0.5°$, $f_\alpha = 45$ Hz, and $\Delta\alpha = 0.2°$.

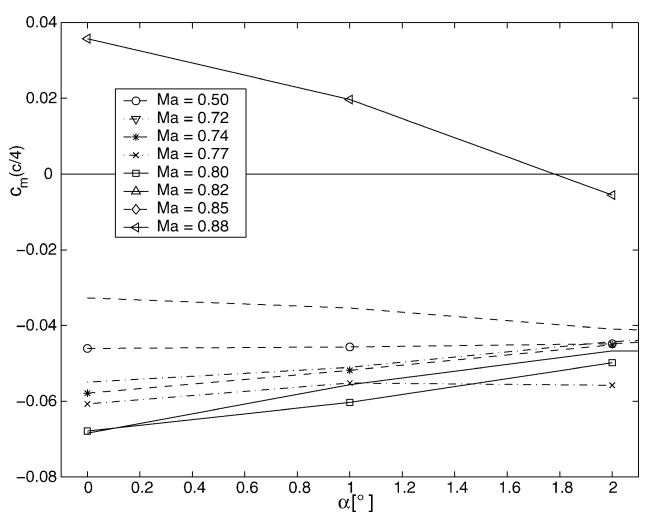

Fig. 11. Pitching moment coefficient depending on the angle of attack from steady pressure measurements.

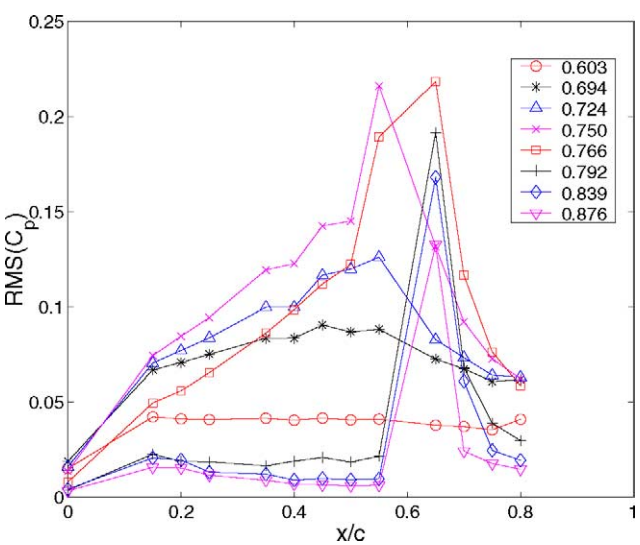

Fig. 13. Fluctuations of the upper surface pressure coefficients for different Mach numbers at $\bar{\alpha} = -0.5°$, $f_\alpha = 90$ Hz, and $\Delta\alpha = 0.2°$.

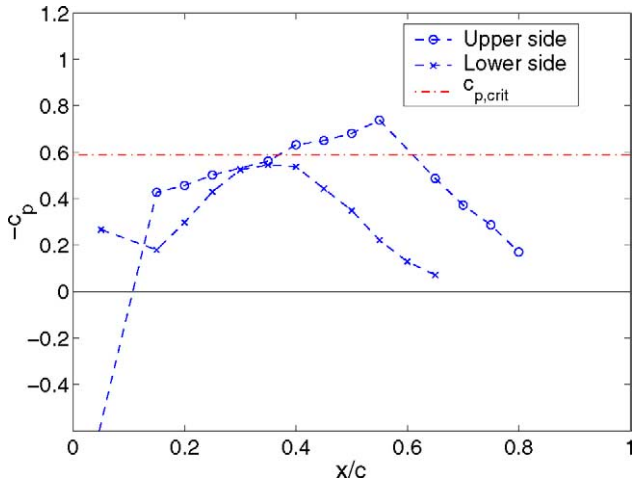

Fig. 14. Time-averaged pressure distribution for $Ma = 0.75$, $\bar{\alpha} = -0.5°$ and $\Delta\alpha = 0.2°$. $\omega^* = 0.17$.

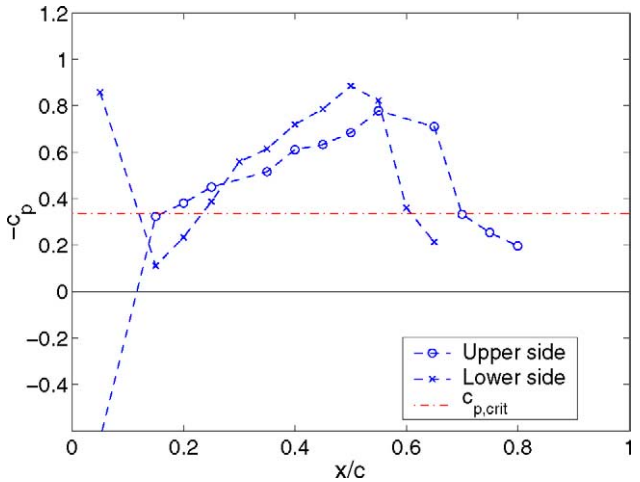

Fig. 16. Time-averaged pressure distribution for $Ma = 0.84$, $\bar{\alpha} = -0.5°$ and $\Delta\alpha = 0.2°$. $\omega^* = 0.16$.

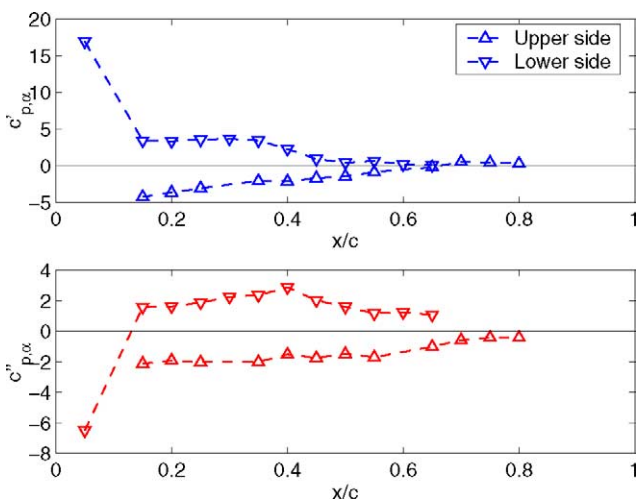

Fig. 15. Unsteady pressure distribution for $Ma = 0.75$, $\bar{\alpha} = -0.5°$ and $\Delta\alpha = 0.2°$. $\omega^* = 0.17$.

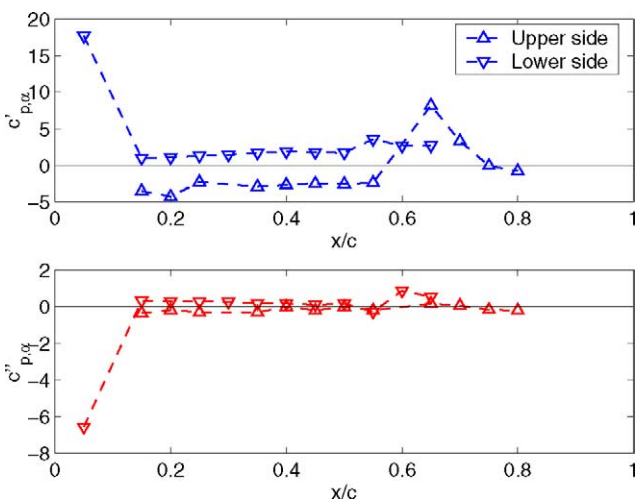

Fig. 17. Unsteady pressure distribution for $Ma = 0.84$, $\bar{\alpha} = -0.5°$ and $\Delta\alpha = 0.2°$. $\omega^* = 0.16$.

only the case in the region of the shock but overall on the upper side. Since this is likely due to a higher fluctuation level of the incoming flow, one should be careful with an (over)interpretation at this point.

The interaction between the pitching motion and the airfoil flow can be studied by means of the unsteady pressure distributions. For Mach numbers of 0.75 and 0.84, respectively, and a mean angle of attack of $-0.5°$, Figs. 14 and 16 show the time-averaged and Figs. 15 and 17 the corresponding unsteady pressure distributions with respect to the pitching motion. They are determined from a cross spectral analysis of the recorded time signals of the pressure and the pitching motion $\alpha(t)$ in radians. The real part is in phase with the pitch oscillations and the imaginary part is shifted by 90°.

In the first case (Figs. 14, 15) the unsteady pressure distribution does not show significant local extrema or slope changes except for the sign change of both parts on the upper side in the region of the shock. The imaginary part also has a local minimum over there.

The second case for the higher Mach number still shows an in-phase relationship in the upper forward airfoil region but an even stronger effect of the pitching motion on the upper and lower airfoil surface pressure distribution in the region of the shocks. Due to a failure of the sensor at 60% chord on the upper side the values at that position are unknown. Nevertheless it can clearly be derived from the signals of both adjacent sensors that the sign of the real part changes due to the shock movement on the oscillating airfoil. This explicit sign change at the location of the shock in connection with a local maximum can be observed at Mach numbers above 0.79 which corresponds with the change in the slope of the damping coefficient observed during the free oscillation tests.

4. Summary

This paper describes the experimental setup for the measurement of unsteady pressures and forces on a rectangular wing section oscillating in pitch and gives an overview on the measured steady and unsteady aerodynamic data in two-dimensional transonic flow. The results of steady pressure measurements with a fixed model are presented as background information for a better understanding of the unsteady flow around the supercritical airfoil undergoing free and forced pitch oscillations. During the experiments with decaying oscillations of the elastically mounted wing section no unstable case was found but a trend of the determined damping coefficient could be observed that leads to the assumption of a torsional instability at Mach numbers above 0.85. The behaviour of the steady pitching moment and lift slope were invoked as possible explanation. The analysis of the forced pitch oscillations concentrated on fluctuations of the airfoil pressure distribution as well as on the unsteady pressure coefficients. Some assumptions were made concerning the influence of flow separation, again with the aid of steady data.

Acknowledgements

The experiments are carried out at the *Aerodynamisches Institut Aachen* within the frame of the collaborative research centre SFB 401 of the *Rheinisch-Westfälische Technische Hochschule Aachen*: "Modulation of Flow and Fluid–Structure Interaction at Airplane Wings".

We are especially grateful to the scientists of *DLR Göttingen, Institut für Aeroelastik* [7,8] for the most appreciated cooperation. We got ongoing advice and valuable input for the project particularly concerning the experimental setup and the general configuration.

References

[1] J. Amecke, Direkte Berechnung von Wandinterferenzen und Wandadaption bei zweidimensionaler Strömung in Windkanälen mit geschlossenen Wänden, DFVLR-FB 85-62, 1985.

[2] M. Drela, Two-dimensional transonic aerodynamic design and analysis using the Euler equations, PhD thesis, Massachusetts Institute of Technology, 1985.

[3] C. Hillenherms, W. Limberg, W. Schröder, Experimental setup for transonic flow over a 2-D rectangular wing section oscillating in pitch, in: Proc. 22nd Congress of the International Council of the Aeronautical Sciences, Harrogate, UK, 27 August–1 September 2000. ICAS-2000-3.1.3.

[4] C. Hillenherms, W. Schröder, W. Limberg, Unsteady force and pressure measurements on an oscillating rectangular wing section in transonic flow, in: Proc. 19th AIAA Applied Aerodynamics Conference, Anaheim CA, 11–14 June, 2001. AIAA Paper 2001-2468.

[5] K. Hufnagel, Entwicklung und Optimierung von Sechs-Komponenten-DMS-Windkanalwaagen zum Einsatz unter kryogenen Bedingungen, Dissertation, TH Darmstadt, 1995.

[6] H.-J. Romberg, Experimentelle Untersuchung der schallnahen Umströmung eines superkritischen Tragflügelprofils unter besonderer Berücksichtigung von Windkanalinterferenzen, Dissertation, RWTH Aachen, März 1990.

[7] G. Schewe, H. Deyhle, Experiments on transonic flutter of a two-dimensional supercritical wing with emphasis on the non-linear effects, in: Proceedings of the Royal Aeronautical Society Conference on "Unsteady Aerodynamics", 17–18 July 1996.

[8] G. Schewe, A. Knipfer, H. Mai, G. Dietz, Experimental and numerical investigation of nonlinear effects in transonic flutter, DLR IB 232-2002 J 01, 2002.

[9] G. Schewe, H. Mai, G. Dietz, Nonlinear effects in transonic flutter with emphasis on manifestations of limit cycle oscillations, J. Fluids Structures 18 (1) (2003) 3–22.

[10] R. Voß, Wall correction methods for dynamic tests, in: AGARDograph 336: Wind Tunnel Wall Corrections, NATO AGARD, 1998, pp. 1–29.